Pergamon

Available online at www.sciencedirect.com
SCIENCE DIRECT®

Cement and Concrete Research 33 (2003) 1407–1415

CEMENT AND CONCRETE RESEARCH

Quality of steel–concrete interface and corrosion of reinforcing steel

T.A. Soylev, R. François*

LMDC INSA/UPS, 135 Avenue de Rangueil, 31077 Toulouse Cedex 4, France

Received 21 November 2002; accepted 24 February 2003

Abstract

This article deals with the influence of steel–concrete interface defects on reinforcing steel corrosion. The defects that are analyzed in this paper relate to the gaps caused by bleeding, settlement and segregation of fresh concrete under horizontal reinforcing bars. These defects are increasing with the concrete depth below the horizontal reinforcement and depend on the bleeding capacity of concrete mixture. Various concrete mixtures including self-compacting concrete (SCC) were tested. The defects at the interface were characterized by the ultimate bond strength recorded in a pullout test and by the defect length under the reinforcement measured with a videomicroscope. The results indicate a good correlation between these two characterization methods. The corrosion was measured by the resistance of polarization and corroded surface area. The results allow us to conclude that the quality of concrete and steel–concrete interface, decreasing with height of concrete section, affects directly the corrosion rate.

Keywords: Corrosion; Reinforcement; Bleeding; Bond strength; Self-compacting concrete

1. Introduction

The reinforcing steel is in a passive state in concrete due to the high pH level of the cement paste. In chloride environment, the initiation of corrosion occurs only when the chloride content is higher than the chloride threshold value. This value calculated per cement mass or per the ratio of chlorides to hydroxides has been taken as a constant value by many authors [1,2], but the experimental results from different researchers reveal an important discrepancy for the chloride threshold value [1–4]. For example, an alkaline solution with the same pH level of concrete does not have the same protection against corrosion [1–6]. A good adhesion between steel and concrete provides better protection to steel [2–13]. Hydration products form a lime-rich layer on the steel surface [5–7,13–16], which restrains the pH drop by the buffering effect against acidification caused by the hydrolysis of iron in pitting corrosion [2,3,5–7,13–16]. It also limits the cathodic reaction by covering the surface of steel available for oxygen [5]. The dense concrete with a good adhesion to steel blocks the diffusion away from corrosion products, and therefore make repassivation easier [8]. The movement of chlorides at the interface is limited by the dense concrete [8]. Consequently, the occurrence of active corrosion of steel in concrete is determined by the presence of voids at the steel–concrete interface [6,8,11,12]. One common type of defect at the steel–concrete interface is the formation of voids under the steel bars oriented perpendicularly to the casting direction of fresh concrete. The rising bleed water can be trapped under the reinforcement. The fresh concrete settles under the steel bar leaving an air void and bleed water collects easily [10]. Corrosion occurs in areas where the steel is not in contact with concrete. The amount of bleeding increases with sample depth and, as a result, the bond strength, which is a function of the interface between steel and concrete, decreases with the sample depth [10–13,17–23]. This effect is recognized in design codes by applying a correction factor to increase the anchorage length. Eurocode 2 [24] and ACI 318R-95 [25] require the increase of development lengths by 43% and 30%, respectively, when the concrete depth below horizontal bar is more than 25 and 30 cm. This effect increases with increasing slump for conventional concrete [23], but self-compacting concrete (SCC), which has a high slump, exhibits a good stability [13,19,20,22,26]. The combination of high-range water reducer (HRWR) and viscosity-modifying admixture (VMA) enables high fluidity

* Corresponding author. Tel.: +33-5-61-55-9905; fax: +33-5-61-55-9900.

E-mail address: raoul.francois@insa-tlse.fr (R. François).

0008-8846/03/$ – see front matter © 2003 Elsevier Ltd. All rights reserved.
doi:10.1016/S0008-8846(03)00087-5

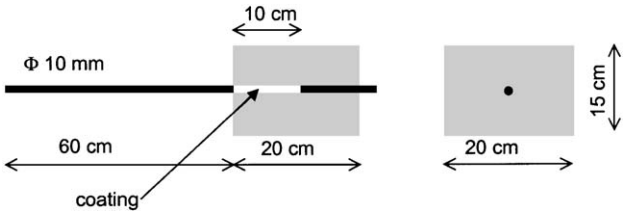

Fig. 1. Samples obtained by sawing the columns.

and high stability [19,20]. As a result, SCC resists to bleeding and settlement in spite of its high slump. The stability may also be increased with the use of fine materials such as silica fume [19,20]. It is noteworthy that the durability and mechanical performance of concrete are reduced with the increase in water–cement (w/c) ratio and permeability due to bleeding and sedimentation of fresh concrete [13,20,27–29]. This effect contributes to the increase in corrosion and to the decrease in bond strength with sample depth already caused by the decrease of steel–concrete interface quality.

This paper analyses the influence of defects at the steel–concrete interface caused by bleeding of fresh concrete on reinforcement corrosion. The variation of steel–concrete bond together with the variation of concrete quality along a vertical concrete section of normal to SCC of various bleeding capacity has been compared.

2. Experimental program

A plywood formwork, 200 cm high and with a 20 × 20-cm cross section, was used to cast the five experimental column elements. Each column had 13 reinforcing bars that were placed horizontally and rigidly fixed. The distances from the bottom of the columns to the center of the reinforcing bars were varying from 10 to 190 cm. The center-to-center spacing between adjacent bars was 15 cm. Plain round steel bars with a 10-mm diameter were used.

The columns were removed from the mould after 6 days and cured at a 100% relative humidity during 28 days before sawing to obtain 13 samples per column, with the steel bar at the center of each sample (Fig. 1).

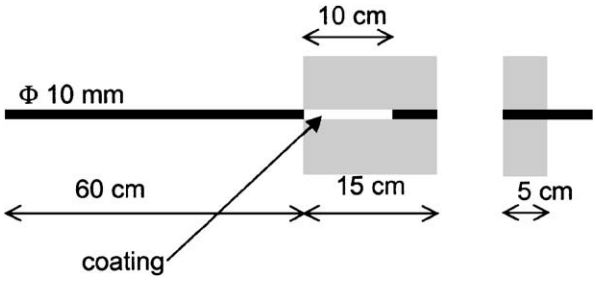

Fig. 2. Samples after sawing: the 15-cm part was used for pullout test and the other part to study the steel–concrete interface and corrosion at videomicroscope.

Table 1
Mixture proportions

Materials (kg/m^3)	C20	C40	SCC40	C50	SCC50
CPA CEM I 52.5 PM ES CP2	304	365.5		430	450
CPA CEM I 52.5 CP2			310		
Silica fume					30
Total water	229	195	186	167	186.9
Sand 3.15 R			490		
Sand 0/4 C			330		
Sand 0/4 R					728
Sand 0/5 R	990	736		780	
Coarse aggregate 4/10 C			460		
Coarse aggregate 4/10 R					992
Coarse aggregate 10/14 C			360		
Coarse aggregate 5/15 R	862	1117		1020	
Limestone filler			140		
Viscocrete 2100 (plasticizer)					3.84
Viscocrete 3010 (VMA–HRWR)			4.05		7.68
Plastiment HP (plasticizer)			1.8		
Sikatell 200 (VMA)			1.28		
Glénium 27 (superplasticizer)				8.6	
Water/cementitious materials ratio	0.75	0.53	0.60	0.39	0.39

Then, each sample was sawed into two pieces of 15 and 5 cm (Fig. 2), to be tested mechanically (pullout test) and observed by a videomicroscope. The sample, 5 cm wide, was also used to obtain cores with a diameter of 6 cm for corrosion measurement. The part of steel, which was not embedded in concrete, and also the top and bottom surfaces of concrete cores were covered with an epoxy resin.

Concrete cores with 3.5-cm diameter and 5-cm height, taken on column perpendicularly to the casting direction at the level of each bar, were used to measure compressive strength, density and porosity (open porosity measured by water saturation) of concrete.

2.1. Concrete mixture proportions

Five different mixtures of concrete were used (Table 1): C20, C40, SCC40, C50 and SCC50. The mixtures were named with respect to compressive strength (20, 40 and 50 MPa). C stands for vibrated concrete and SCC stands for self-compacting concrete.

2.2. Materials

The cement used for SCC40 was a French portland cement (CPA-CEMI 52.5 CP2). For the other mixtures, a

Table 2
Physical properties of cement

	CPA CEMI 52.5 PM ES CP2	CPA CEMI 52.5 CP2
Density	3.15	3.15
Blaine (cm^2/g)	3700	4400

Table 3
Oxide composition of cements

	Chemical analysis (percentage by mass)								
	SiO_2	Al_2O_3	Fe_2O_3	CaO	MgO	K_2O	Na_2O	SO_3	Loss of ignition
CPA CEMI 52.5 PM ES CP2	21.26	3.57	4.36	64.61	0.98	0.24	0.12	2.7	1.11
CPA CEMI 52.5 CP2	20.72	4.52	2.98	64.63	1.87	0.91	0.08	3.46	0.70

French portland cement (CPA-CEMI 52.5 PM ES CP2) with a low-C_3A content (sulfate resistant) was used. The physical and chemical properties of the cements are given in Tables 2–4. The silica fume used had a specific surface of 15 m^2/g. The particle size of the limestone filler was 0/0.1 mm (85% of particles <0.08 mm).

2.2.1. Admixtures

The Plastiment HP is a plasticizer of high performance of Sika. The Sika Viscocrete 2100 is a plasticizer water-reducing admixture. The Sika Viscocrete 3010 SCC is a superplasticizer for SCC, and moreover, it has a viscosity-enhancing effect. The Sikatell 200 VP is a cohesiveness-enhancing admixture and the Glenium 27 of MBT is a superplasticizer.

All mixtures were prepared in 110-l batches among which 80 l were intended for the column and the remainder for the fresh and hardened concrete tests.

2.3. Testing program

Slump, slump flow, density and entrapped air of fresh concrete were measured. Compressive and tensile strength (splitting test) at 28 days were measured by cylindrical samples 220 mm high and with a diameter of 110 mm (Tables 5 and 6).

2.3.1. Pullout test

A plastic sheathing of 10 cm was attached to the loaded end of each bar to limit the bond between the bar and concrete to 5 cm (Fig. 1). The pullout load versus slip was recorded. The ultimate bond strength, which gives the point of steel–concrete rupture for round bars, was calculated by Eq. (1):

$$\tau = P/\pi dl \quad (1)$$

where P, d and l correspond to the applied load, bar diameter and anchored length, respectively.

Table 4
Percentages of main compounds according to Bogue's equations

	C3S	C2S	C3A	C4AF
CPA CEMI 52.5 PM ES CP2	63.5	13.2	2.1	13.3
CPA CEMI 52.5 CP2	61.1	13.4	7.0	9.1

Table 5
Tests on fresh concrete

	C20	C40	SCC40	C50	SCC50
Slump (cm)	15.8	7.6		23	
Slump flow (cm)			63		60
Entrapped air (%)	2	1.4	2.2	1.4	1.8
Density	2.38	2.43	2.33	2.48	2.41

2.3.2. Videomicroscope

Steel–concrete interface was analyzed by a videomicroscope with an enlargement of 25 and a magnification of $\times 175$. The areas of defects were quantified in terms of steel length not bounded to concrete at the lower part of the bar due to bleeding and settlement (Fig. 3).

2.3.3. Corrosion measurements

The concrete cores used to measure corrosion were completely dried at 50 °C to enhance capillary suction prior to the first immersion. For each wetting–drying cycle, the samples were immersed in the 35-g/l NaCl solution for 1 week and then kept in room conditions for 4 weeks. The corrosion rate of reinforcing steel was measured by the resistance of polarization at the end of each wetting cycle during 55 weeks. After 55 weeks, the samples were crushed out and the surface area corroded was calculated as a percentage of the total area of steel embedded in concrete. The chloride content at steel–concrete interface was measured for samples at the bottom of each column (denser concrete with lower porosity) to confirm whether the chloride amount was higher than the chloride threshold value for corrosion initiation.

3. Results and discussions

3.1. Effect of height on density and porosity

Figs. 4 and 5 show the density and porosity variation along the column for the five mixtures of concrete tested. Over a height of 40 cm, the density and porosity variation are insignificant along the height. However, at the bottom of the columns (10 cm), there is a denser zone of concrete due to compaction caused by the concrete weight. The porosity of C20 exhibits a slight increase along the height due to its higher bleeding capacity (higher w/c ratio) [10,13,19,20,22,27–29]. Porosity is a function of strength class of concrete and decreases as concrete strength increases.

Table 6
Compressive strength at 28 days (MPa)

	C20	C40	SCC40	C50	SCC50
Compressive strength (MPa)	27.4	45.8	43.9	55.4	57.1
Tensile strength (MPa)	3.0	3.8	3.4	4.4	5.1

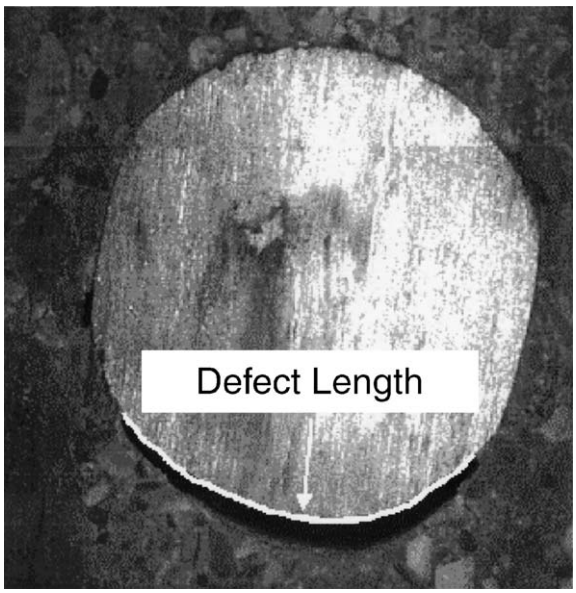

Fig. 3. Steel–concrete interface at a videomicroscope with an enlargement of × 25 magnification.

3.2. Effect of height on compressive strength

Fig. 6 shows the variation of compressive strength along the column height. In spite of a slight decrease tendency along the height, the compressive strength values exhibit an important variation. This dispersion might be due to the axis of core samples, which was perpendicular to the casting direction [13]. Because of this important dispersion, the values of compressive strength were not used to normalize the bond strength values.

3.3. Influence of the height on steel–concrete interface defects

Photos of steel–concrete interface, analyzed by videomicroscope, show that the defect of steel–concrete interface

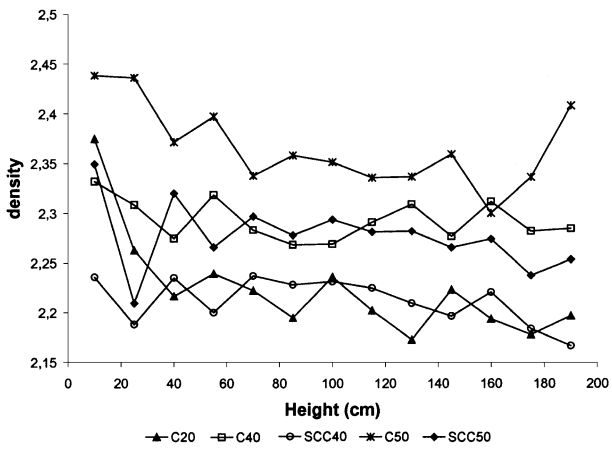

Fig. 4. Variation of density with depth of concrete for the five concrete mixtures tested.

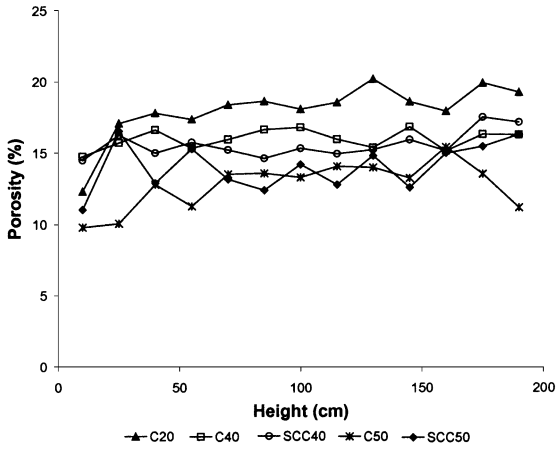

Fig. 5. Variation of porosity with depth of concrete for the five concrete mixtures tested.

at the bottom part of steel, caused by bleeding and settlement, increases along the height (Fig. 7). This defect was quantified by the length of steel, which is not in contact with concrete. Thus, the *defect factor* can be defined as the ratio of the defect length to the bar perimeter.

Unlike the values of compressive strength and porosity, which exhibit a slight decrease along the height and with a similar behavior for various types of concrete, the defect value decreases significantly along the height (Fig. 8), and the rate of this decrease depends strongly on the type of concrete due to its bleeding capacity [10,13,17–20,22,23]. For strength class of 50 MPa, there is no defect at the interface. These concrete have a lower w/c ratio and as a result, bleeding is lower.

For C20, in general, three zones can be observed along the height [10]. Firstly, a compression zone where the concrete is denser near the bottom of the column. Secondly, a zone of constant density at the middle part of the column. Lastly, a zone of clear water where the external bleeding water is collected. The latter is more important

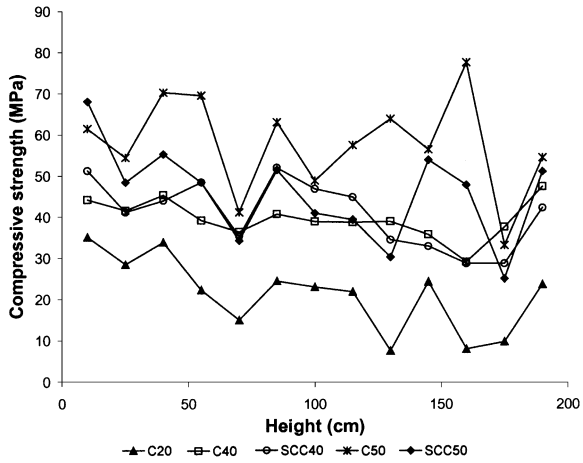

Fig. 6. Variation of compressive strength with depth of concrete for the five concrete mixtures tested.

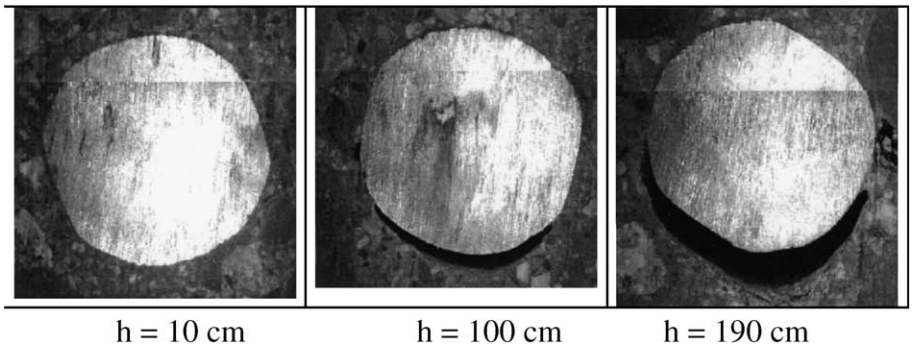

Fig. 7. Three sections of C40 at 10, 100 and 190 cm of height, respectively, at videomicroscope with an enlargement of × 25 magnification.

for C20 in comparison with the other concrete mixtures, and consequently, the compression zone must also be more important. Near the top of column, after 160 cm, a total loss of steel–concrete bond was observed. This region corresponds to the zone of high external bleeding water accumulation. Near the column bottom, there is no defect below 40 cm. Some points between 40 and 160 cm do not include any defect.

For the two concrete mixtures of the same class of strength (40 MPa), the defect values are greater for conventional concrete despite of a higher w/c of the SCC. This result can be explained by the SCC stability because of its special mixture formulation. With the use of viscosity-modifying admixture, limestone filler enhances the bleeding decrease [19,20]. The higher specific surface of the cement and crushed aggregates used for the SCC may have a slight influence on the bleeding decrease [10]. The defects were observed over a height of 25 cm for C40 and over 40 cm for SCC40. For conventional concrete, between 40 and 130 cm, the defect values do not change significantly. Over 130 cm, the defect values are higher because of the rising bleeding water. The behavior of SCC40 is similar, except for some fluctuations.

3.4. Effect of height on bond strength between steel and surrounding concrete

Fig. 9 shows that the ultimate bond strength decreases as a function of the concrete depth below the horizontal bar. Similarly to the behavior of defects along the height, this decrease depends on concrete mixture. The average value of bond strength increases as a function of the strength class of concrete. The concrete type (conventional or SCC) defines the difference of value between the top and the bottom part of the column. The highest decrease of bond strength is observed for C20, which is the conventional concrete with the highest slump: the decrease starts at a height of 40 cm with 54% in relation to the bottom and varies between 56% and 64%, and between 40 and 160 cm up to the total rupture of bond.

Because of the bond strength decrease along the height of concrete section, the anchorage length of the bars located in the upper part of column must be increased so as to maintain a constant bond strength [11–13,17–20,22–25]. The *casting position factor* [23] defines the ratio of the bar bond strength, placed at the bottom part, to the bond strength of a bar placed at another height of the concrete section.

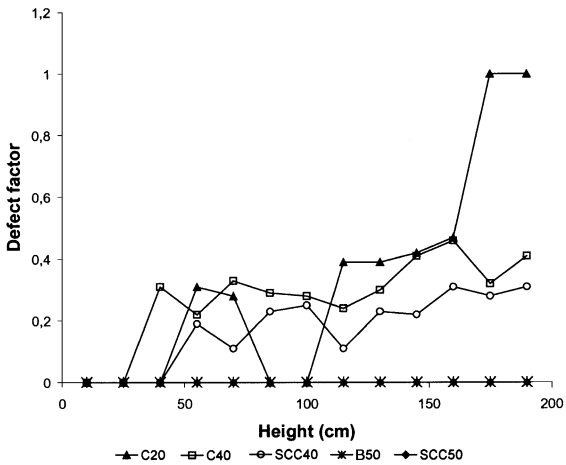

Fig. 8. Variation of the defect factor with concrete depth for the five concrete mixtures tested.

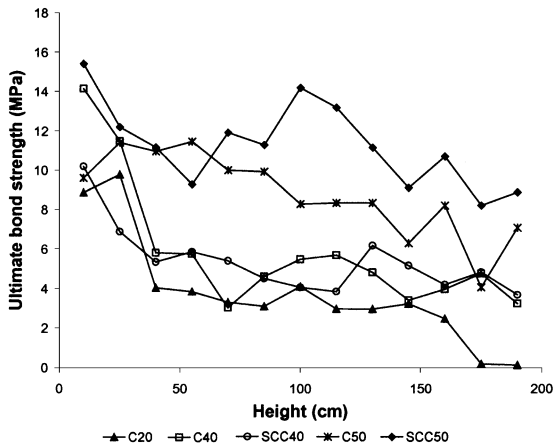

Fig. 9. Variation of the ultimate bond strength with concrete depth for the five concrete mixtures tested.

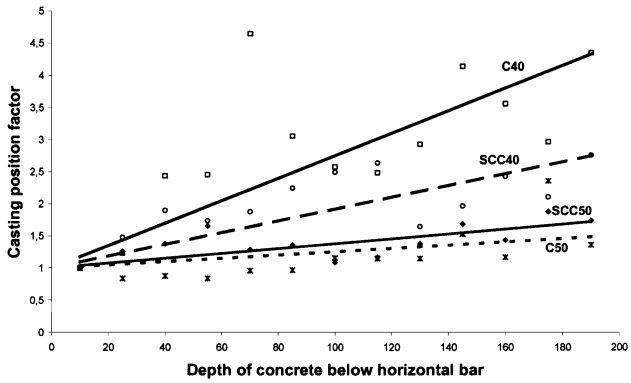

Fig. 10. Variation of the casting position factor with depth of concrete for the five concrete mixture tested.

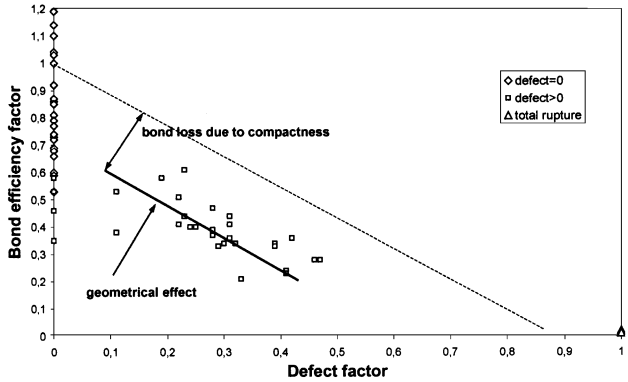

Fig. 12. Correlation between the bond efficiency factor and the defect factor.

Fig. 10 shows the variation of the casting position factor with the depth of concrete below horizontal bars. The linear function of the conventional concrete C40, which has a w/c of 0.53, has a slope 2.2 times of the SCC40s, which has a w/c of 0.60 (this uniformity despite w/c greater, must be due to viscosity-enhancing admixtures and limestone filler), 4.63 times of the SCC50s and 6.77 times of the vibrated C50s, which both have w/c of 0.39. The behavior of C20 is similar to C40s but over 160 cm the bond strength approaches zero, as mentioned before, due to high external bleeding (Fig. 11).

3.5. Correlation between steel–concrete interface defects and the ultimate bond strength

Fig. 12 shows the correlation between the *bond efficiency factor* [23] (the inverse of the casting position factor) and the defect factor. For a significant interval, the bond efficiency factor is linearly proportional to the defect factor. However, near the bottom and the top of the column, there is no proportionality. Near the bottom of the column, because of higher density of concrete, there is a decrease of the bond efficiency factor without variation of the defect factor.

In the middle part of the column, there is a good proportionality between bond strength and steel–concrete interface defect. This proportionality is related to the geometrical effect on the perimeter of steel that is in contact with the surrounding concrete and it does not depend on the type of concrete. This proportionality may be used to foresee the bond strength decrease along the height by the analysis of the defects and vice versa.

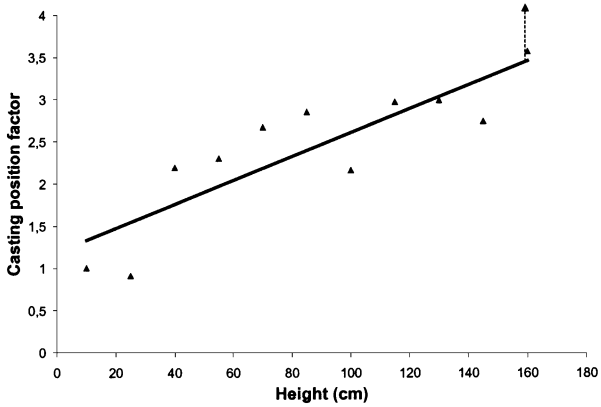

Fig. 11. Variation of the casting position factor with concrete depth for C20.

3.6. Chloride penetration into concrete

In order to check the chloride level at the steel–concrete interface, the total chloride content by weight of cement was measured near the bottom of the column where the concrete is denser and the amount of chlorides is expected to be lower than the top of the column (Table 7).

The amount of chlorides is deemed as critical for the initiation of corrosion when the Cl^-/OH^- ratio varies in interval from 0.6 to 1.0, which corresponds approximately to an interval of 0.2–0.4% by cement weight [1,2]. The values measured at the steel–concrete interface are greater than the threshold value of chlorides for the initiation of corrosion. The chloride content of the SCC40 is higher than the other mixes due to the higher C_3A content of the cement used for this concrete, which leads to an increase of chloride binding.

3.7. Corrosion of steel

Fig. 13 shows the results of R_p measurement obtained after seven cycles of drying–wetting and corresponding to 55 weeks of chloride exposure. In addition to the R_p measurement that gives instantaneous rate of corrosion, the area of surface corroded was also measured after 55 weeks by breaking the samples to observe the total corrosion (Fig. 14).

Table 7
Total chloride content at the vicinity of steel (Clint) and near the surface (Clsur)

	C20	C40	SCC40	C50	SCC50
Clint (percentage of mass of cement)	2.67	2.26	3.08	1.15	1.12
Clsur (percentage of mass of cement)	2.82	2.39	3.23	1.50	1.59

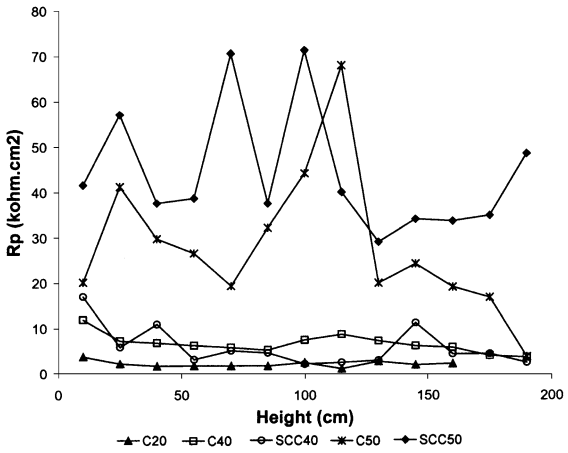

Fig. 13. Variation of the polarization resistance with concrete depth.

The average value of the R_p and corroded surface area results of all the heights shows that the corrosion rate is a function of concrete quality and corrosion increases as the class of concrete strength decreases.

The average value of corroded area of the upper part of steel is lower than that of the lower part by 12% for C20, 10% for C40 conventional, 23% for SCC, 4% for C50 vibrated and 1% for SCC50. These results show the role of defects at the lower part of the reinforcement on the corrosion of less strength concretes.

For the C20, near the column bottom, the value of R_p is greater than the other values. This behavior is similar to the porosity variation (Fig. 15). Near the column bottom, the concrete is denser; therefore, corrosion is weaker. The high chloride content along the height enhances a high corrosion rate, and it is difficult to detect the role of the steel–concrete interface on corrosion. The corrosion rate is important for all reinforcement with or without defects at the interface. It seems that high porosity is a significant defect, which can induce corrosion development.

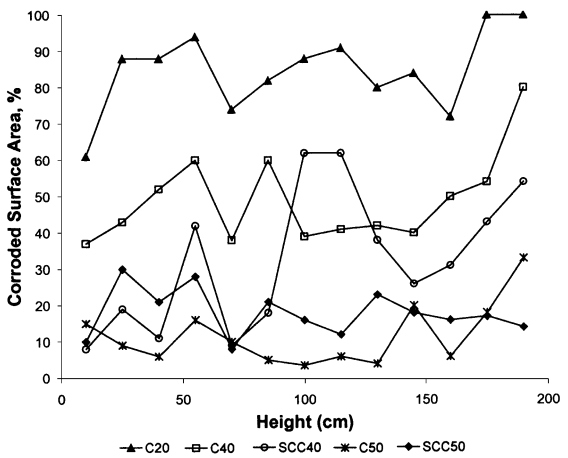

Fig. 14. Variation of the corroded surface area as a percentage of the total surface area of the steel embedded in concrete with concrete depth.

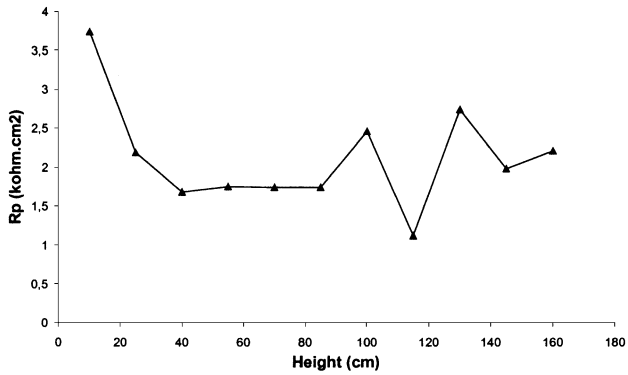

Fig. 15. Variation of the R_p with concrete depth for C20.

For C40, R_P decreases along the column height (Fig. 16). Near the bottom of the column, R_p is greater and corresponds to the compression zone due to concrete settlement. There is a similarity between the behavior of R_p and the ultimate bond strength along the height as shown in Fig. 17, which shows the role of steel–concrete interface on corrosion. The porosity of these concretes is uniform over the column bottom; consequently, the variation of interface quality must be the cause of R_p decrease.

For C50, there is no tendency to decrease or increase for the R_p along the height (Fig. 13). This behavior, which is more uniform in relation to the other concretes, shows the uniformity role of both concrete and steel–concrete interface along the height.

The two major factors, which describe the behavior of R_p along the height, are the increase of concrete porosity and the decrease of steel–concrete interface quality along the height. The porosity of concrete is lower near the column bottom, and over 25 cm it is uniform along the height. Consequently, this cannot explain why R_p has decreased along the height for the C40. The second factor, which is the quality of steel–concrete interface, must explain the decrease of R_p; anyway, the decrease of the ultimate bond strength is very similar to that of the R_p for the C40.

On crushing specimens, crevice corrosion on the electrode surface near the epoxy coating was observed. The corroded

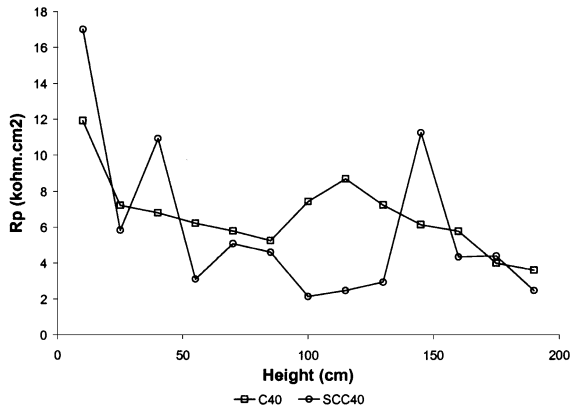

Fig. 16. Variation of the R_p with concrete depth for C40.

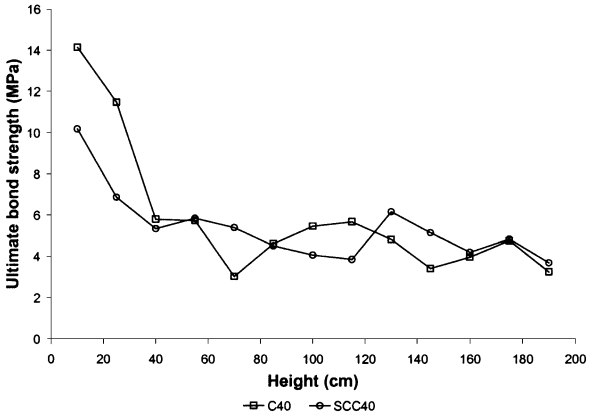

Fig. 17. Variation of the ultimate bond strength with concrete depth for C40.

surface area due to crevice corrosion attack was approximately 25% of the total electrode surface area. If this area is canceled out from the calculation of the total corroded surface area, there will be no corrosion for high-quality concretes, C50 and SCC50, despite the chloride amount, which is greater than the threshold value for the initiation of corrosion. For C20, the corrected corroded surface area will range between 36% and 69% and between 1% and 37% for C40. For SCC40, the corrosion will only occur on some heights of the column and at these heights, the corrosion difference between the upper and the bottom part with respect to casting direction is more important. Consequently, the quality of steel–concrete interface is the major factor to explain the initiation of corrosion [2–8,11–16].

4. Conclusion

This research confirms the presence of defects between steel and concrete under the lower part of the rebar over 25–40 cm for C20 and C40 as recognized in design codes. These defects induce two major consequences.

First of all, they are the cause of the bond strength decrease between steel and concrete along the height of concrete section. The anchorage length of top-cast bars must be multiplied by a factor, which is equal to the ratio of the bottom to top bar bond strength.

Secondly, they enhance the corrosion of reinforcing steel due to the lack of chemical and physical protection supplied by a dense concrete.

The measure of bond strength between steel and concrete allows us to quantify the quality of adhesion steel–concrete (for plain steel), which varies near the bottom as a function of concrete compactness, and then as a function of the intensity of defects of steel–concrete interface. There is a good correlation between the decrease of bond strength and the increase of defect intensity.

The use of various concrete mix proportions has shown the advantage of HRWR and VMA. The conventional concrete with higher slump has a higher bleeding capacity, which causes the decrease of the quality of steel–concrete interface along the concrete section height. The use of HRWR enables to diminish w/c, and the VMA allows to increase the stability of concrete. The addition of supplementary cementing materials such as silica fume is another way to increase the stability of concrete.

The corrosion of concrete increases along the concrete section height. This result, which is in adequacy with the bond strength for C40, shows the quality role of steel–concrete interface on corrosion. For C20, which has a high porosity, the corrosion rate is too high to differentiate the interface influence. For C50, there is no clear tendency. The uniformity of quality of concrete and steel–concrete interface enhances a more uniform protection behavior against corrosion along the concrete section height.

SCC improves the uniformity of physical and mechanical properties along the concrete section height, and as a result, concrete durability increases.

References

[1] C. Alonso, C. Andrade, M. Castellote, P. Castro, Chloride threshold values to depassivate reinforcing bars embedded in a standardized OPC mortar, Cem. Concr. Res. 30 (2000) 1047–1055.
[2] G.K. Glass, N.R. Buenfeld, Chloride threshold levels for corrosion induced deterioration of steel in concrete, in: L.O. Nilsson, J.P. Ollivier (Eds.), Chloride Penetration into Concrete, Proceedings of the International RILEM Workshop, St-Rémy-lès-Chevreuse, 1995, pp. 429–440.
[3] G.K. Glass, The influence of the steel–concrete interface on the risk of chloride induced corrosion, Proceedings of COST 521 Workshop Annecy project UKG, 1999, pp. 1–8.
[4] A. Castel, R. François, G. Arliguie, Factors other than chloride level influencing corrosion rate of reinforcement, in: V.M. Malhotra (Ed.), CANMET/ACI Durability of Concrete, Barcelona, 2000, pp. 629–644.
[5] C.L. Page, Mechanism of corrosion protection in reinforced concrete marine structures, Nature 258 (11) (1975) 514–515.
[6] P. Lambert, C.L. Page, P.R.W. Vassie, Investigations of reinforcement corrosion: 2. Electrochemical monitoring of steel in chloride-contaminated concrete, Mat. Struct. 24 (1991) 351–358.
[7] C.L. Page, K.W.J. Treadaway, Aspects of the electrochemistry of steel in concrete, Nature 297 (1982) 109–115.
[8] T. Yonezawa, V. Ashworth, R.P.M. Procter, Pore solution composition and chloride effects on the corrosion of steel in concrete, Corros. Eng. 44 (7) (1988) 489–499.
[9] G.E. Monfore, G.J. Verbeck, Corrosion of prestressed wire in concrete, J. Am. Concr. Inst. 32 (5) (1960) 491–515.
[10] S.H. Kosmatka, Bleeding significance of tests and properties of concrete and concrete making material, in: ASTM Special Publication, Philadelphia, STP 169C, 1994, pp. 88–111.
[11] T.U. Mohammed, N. Otsuki, M. Hisada, Corrosion of steel bars with respect to orientation in concrete, ACI Mater. J. 96 (2) (1999) 154–159.
[12] T.U. Mohammed, H. Hamada, A discussion of the paper "Chloride threshold values to depassivate reinforcing bars embedded in a standardized OPC mortar" by C. Alonso, C. Andrade, M. Castellote, and P. Castro, Cem. Concr. Res. 31 (2001) 835–838.
[13] N. Petrov, Etude des propriétés d'un béton autonivelant in situ et de leurs influences sur l'interface béton-armature, Masters Thesis, Université de Sherbrooke, 1998.
[14] A.K. Suryavanshi, J.D. Scantlebury, S.B. Lyon, Corrosion of reinforcement steel embedded in high water–cement ration concrete contaminated with chloride, Cem. Concr. Compos. 20 (1988) 263–281.

[15] G.K. Glass, N.R. Buenfeld, Differential acid neutralisation analysis, Cem. Concr. Res. 29 (1999) 1681–1684.
[16] G.K. Glass, B. Reddy, N.R. Buenfeld, Corrosion inhibition in concrete arising from its acid neutralisation capacity, Corros. Sci. 42 (2000) 1587–1598.
[17] G.B. Welch, B.J. Patten, Bond strength of reinforcement affected by concrete sedimentation, J. Am. Concr. Inst. 62 (2) (1965) 251–263.
[18] B. Brettmann, D. Darwin, R.C. Dohaney, Bond of reinforcement to superplasticized concrete, ACI J. (1986 January–February) 98–107.
[19] K.H. Khayat, Use of viscosity-modifying admixture to reduce top-bar effect of anchored bars cast with fluid concrete, ACI Mater. J. 95 (2) (1998) 158–167.
[20] K.H. Khayat, K. Manai, A. Trudel, In situ mechanical properties of wall elements cast using self-consolidating concrete, ACI Mater. J. 94 (6) (1997) 491–500.
[21] V.A. Ghio, P.J.M. Monteiro, Bond strength of reinforcing bars in reinforced shotcrete, ACI Mater. J. 94 (2) (1997) 111–118.
[22] T.A. Söylev, R. François, Défauts d'adhérence acier-béton dus au ressuage et au tassement du béton frais, Ann. Bâtim. Trav. Publics, (6) (2001 December) 25–34.
[23] J.O. Jirsa, J.E. Breen, Influence of casting position and shear development and splice length-design recommendations, Research Report 242-3F, Center for Transportation Research, University of Texas Austin (1981 November).
[24] Eurocode 2: Design of concrete structures: Part 1. General rules and rules for buildings (2001).
[25] ACI 318: Building code requirements for structural concrete (ACI 318-95) and commentary (ACI 318R-95), ACI Committee 318 Standard Building Code, ACI (1996).
[26] W. Zhu, P.J.M. Bartos, Application of depth-sensing microindentation testing to study of interfacial transition zone in reinforced concrete, Cem. Concr. Res. 30 (2000) 1299–1304.
[27] M. Hoshino, Relationship between bleeding, coarse aggregate, and specimen height of concrete, ACI Mater. J. 86 (2) (1989) 185–190.
[28] J.C. Gibbs, W. Zhu, Strength of hardened self-compacting concrete, in: Å. Skarendahl, Ö. Petersson (Eds.), 1st International RILEM Symposium on Self-Compacting Concrete, RILEM Publications S.A.R.L., Stockholm, 1999, pp. 199–210.
[29] W. Zhu, J.C. Gibbs, P.J.M. Bartos, Uniformity of in situ properties of self-compacting concrete in full-scale structural elements, Cem. Concr. Compos. 23 (2001) 57–64.